JACC Vol. 28, No. 7
December 1996:1818–26

Improved Measurement of Pressure Gradients in Aortic Coarctation by Magnetic Resonance Imaging

JOHN N. OSHINSKI, PHD, W. JAMES PARKS, MD,* CHRISTOS P. MARKOU, PHD, HARRIS L. BERGMAN, MS,† BLAKE E. LARSON, MS,† DAVID N. KU, MD, PHD,† SRINIVASAN MUKUNDAN, JR., PHD, MD, RODERIC I. PETTIGREW, PHD, MD

Atlanta, Georgia

Objectives. **This study evaluated whether magnetic resonance imaging (MRI) and magnetic resonance (MR) phase velocity mapping could provide accurate estimates of stenosis severity and pressure gradients in aortic coarctation.**

Background. **Clinical management of aortic coarctation requires determination of lesion location and severity and quantification of the pressure gradient across the constricted area.**

Methods. **Using a series of anatomically accurate models of aortic coarctation, the laboratory portion of this study found that the loss coefficient (K), commonly taken to be 4.0 in the simplified Bernoulli equation $\Delta P = KV^2$, was a function of stenosis severity. The values of the loss coefficient ranged from 2.8 for a 50% stenosis to 4.9 for a 90% stenosis. Magnetic resonance imaging and MR phase velocity mapping were then used to determine coarctation severity and pressure gradient in 32 patients.**

Results. **Application of the new severity-dependent loss coefficients found that pressure gradients deviated from 1 to 17 mm Hg compared with calculations made with the commonly used value of 4.0. Comparison of MR estimates of pressure gradient with Doppler ultrasound estimates (in 22 of 32 patients) and with catheter pressure measurements (in 6 of 32 patients) supports the conclusion that the severity-based loss coefficient provides improved estimates of pressure gradients.**

Conclusions. **This study suggests that MRI could be used as a complete diagnostic tool for accurate evaluation of aortic coarctation, by determining stenosis location and severity and by accurately estimating pressure gradients.**

(J Am Coll Cardiol 1996;28:1818–26)

Coarctation of the aorta is a congenital malformation in which constriction of the aorta causes hypertension proximally and reduces blood flow distally. Clinical management depends on identifying the location and severity of the coarctation and determining the pressure gradient across the lesion. If the stenosis is severe or the pressure gradient is large, or both, surgical intervention or balloon angioplasty is required (1,2). Currently, X-ray angiography is the most common method of locating the aortic coarctation. X-ray angiography requires cardiac catheterization, injection of contrast dye and sedation and necessitates exposing the patient to ionizing radiation. The use of X-ray angiography is especially problematic if multiple follow-up examinations after surgical repair are needed. Patients with coarctation require close postsurgical follow-up because restenosis after angioplasty and development of aneurysm after patch graft repair are not uncommon (3–6).

Transthoracic duplex Doppler ultrasound can be used to evaluate aortic coarctation, but consistent results are difficult to achieve because of problems with obtaining a clear acoustic window, interference from lung tissue and difficulties in determining the throat diameter of the coarctation (7–9). An advantage of ultrasound is that it can be used to obtain an estimate of the pressure gradient across coarctations. Pressure gradient estimates are obtained using throat velocity measurements in the simplified Bernoulli equation

$$\Delta P = KV_t^2, \quad [1]$$

where ΔP is the pressure gradient across the coarctation (mm Hg), V_t the throat velocity (m/s) and K the loss coefficient, often referred to as the Bernoulli coefficient (mm Hg-s^2/m^2), which is commonly taken to be 4.0.

Pressure gradient estimates from the simplified Bernoulli equation are not always accurate because of several assumptions. The simplified Bernoulli equation assumes that the velocity proximal to the stenosis is negligible. This assumption is reasonable for severe stenoses (>75%), and errors may be corrected in mild stenoses by accounting for the proximal

From the Departments of Radiology and Hematology, Emory University School of Medicine; *Children's Heart Center, Egleston Children's Hospital; and †School of Mechanical Engineering, Georgia Institute of Technology, Atlanta, Georgia. This study was supported in part by Grants HL09075 and HL42021 from the National Heart, Lung, and Blood Institute, National Institutes of Health, Bethesda, Maryland and by a grant from Philips Medical Systems, Best, The Netherlands.

Manuscript received May 14, 1996; revised manuscript received July 16, 1996, accepted August 14, 1996.

Address for correspondence: Dr. John N. Oshinski, Frederik Philips MR Research Center, Department of Radiology, Emory University of School of Medicine, 1364 Clifton Road, Atlanta, Georgia 30322. E-mail: oshinski@turlubuki.eushc.org.

Published by Elsevier Science Inc.

0735-1097/96/$15.00
PII S0735-1097(96)00395-6

Abbreviations and Acronyms

ECG = electrocardiographic
MR = magnetic resonance
MRI = magnetic resonance imaging
3D = three-dimensional

velocity (10). However, there are other assumptions in the Bernoulli equation that cannot be easily corrected:

1. The simplified Bernoulli equation assumes that a pressure distal to a stenosis remains at a constant value, equal to the pressure at the throat of the stenosis. In reality, this assumption is true only for a narrow range of stenoses with severity of ~75%. For stenoses with severity <75%, some pressure recovery occurs past the throat of the stenosis (11). The simplified Bernoulli equation (equation 1) will not account for this pressure recovery and hence will overestimate stenosis severity in mild constrictions. Experimental studies have shown (11) that pressure gradients will be overestimated by as much as 30% in mild constrictions.

2. For more severe stenoses, high levels of turbulence are present in the flow field distal to the throat of the stenosis, and the turbulence causes an irrevocable pressure loss that continues past the throat of the stenosis (10,12,13). The simplified Bernoulli equation will not account for this secondary pressure loss and hence will underestimate stenosis severity (9). Experimental studies of stenotic heart valves have shown (9,11) that for severe stenoses (>85%), the simplified Bernoulli equation will underestimate the pressure gradient. These theoretic and experimental studies indicate that the loss coefficient, commonly taken to be a constant value of 4.0, is actually a function of the severity of the stenosis. Figure 1 illustrates a qualitative graph of pressure versus position in the stenosis and shows pressure recovery in mild stenoses and turbulent pressure loss in severe stenoses.

3. The shape of the stenosis is another factor that can cause errors in the pressure gradient estimates using the simplified Bernoulli equation. A sharp-edged orifice-type stenosis will resemble a free jet, and levels of turbulence intensity and pressure recovery distal to the stenosis will be different from that found in a smoothly varying stenosis, which resembles a confined jet (11,13). Therefore, in addition to dependence on stenosis severity, the shape of the stenosis will also affect the value of the loss coefficient.

Use of loss coefficients based on stenosis severity would require that the velocity and vessel diameter at the throat of the stenosis be accurately known. Magnetic resonance imaging (MRI) is a noninvasive imaging modality that is now being used extensively to evaluate vascular disease (14–17). In addition to visualizing vessel lumens, magnetic resonance (MR) phase velocity mapping techniques can create quantitative images of blood flow velocities. Consequently, flow velocities at the throat of the stenosis can be determined using MR phase velocity mapping. Magnetic resonance phase velocity mapping has been used to measure velocities in high flow stenotic lesions, such as aortic valve stenosis, and the technique has proved to be accurate (18,19). Several previous studies have used MRI for evaluation of aortic coarctation. These studies have shown (3,7,8,17) that MRI is superior to ultrasound in determining the location of coarctations and compares well with X-ray angiography in estimating coarctation severity. Because MRI can measure the velocities in the throat and can make accurate images of the vessel diameter, it could be used to more accurately determine pressure decreases across aortic coarctations using values of loss coefficients based on stenosis severity.

The purpose of the present study was to conduct a controlled laboratory study of models of aortic coarctation to

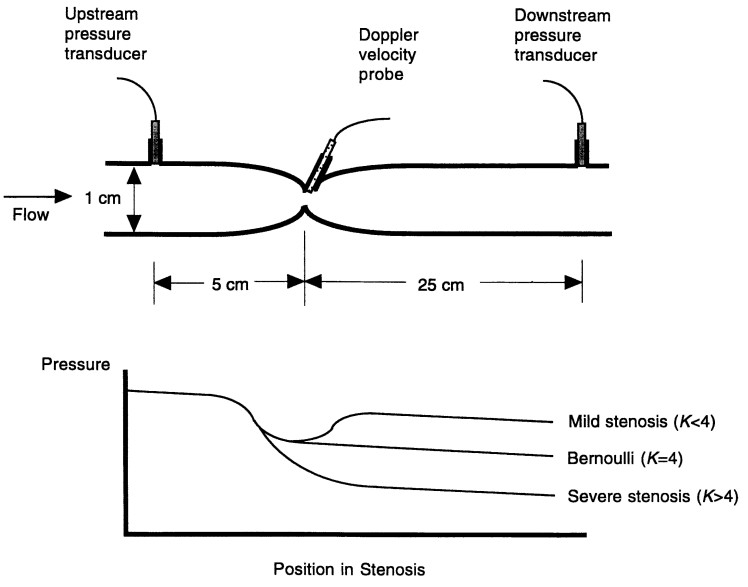

Figure 1. Pressure gradient in stenosis and diagram of coarctation flow model. **Upper diagram** shows the stenosis model, and the **lower graph** illustrates pressure as a position in the stenosis. Along the stenosis in the direction of flow, a small pressure loss due to frictional viscous losses occurs (this is the reason for the slight downward slope on the first portion of the curve in the graph). Near the throat of the stenosis, velocity increases, and pressure decreases. Distal to the stenosis, several possible scenarios may occur, depending on the severity of the stenosis. If the stenosis is mild, significant (even complete) pressure recovery may occur. For these mild stenoses, the loss coefficient K is <4.0. If the stenosis is moderate, turbulent energy loss will cause the pressure distal to the stenosis to remain approximately equal to the pressure at the throat of the stenosis. This is the case for the Bernoulli relation where the loss coefficient K is equal to 4. If the stenosis is severe, turbulent energy losses may be great enough to cause the pressure to drop below its value at the throat of the stenosis. In this case the loss coefficient K is >4.0. The flow model was based on a series of biplane angiograms of aortic coarctations. A Doppler velocity probe was used to measure the throat velocity, and pressure transducers were used to measure the pressure gradient across the stenosis.

determine loss coefficients as a function of stenosis severity and to apply the new loss coefficients to estimate pressure gradient in a series of patients. Peak systolic pressure gradients were calculated with MRI in 32 patients using the new *severity-based* loss coefficients and versus 1) MRI pressure gradient estimates calculated with the commonly used loss coefficient value of 4.0; and 2) Doppler ultrasound estimates of pressure gradient or invasive catheter pressure measurements, or both.

Methods

Flow models. To accurately quantify the loss coefficients in aortic coarctation, an in vitro laboratory model study was designed to consider the geometry and fluid flow characteristics. Six glass tube models were constructed on the basis of a series of biplane angiograms of aortic coarctations. The models had coarctations with severities of 50%, 55%, 60%, 70%, 80% and 90% by diameter. The upstream and downstream diameters were 25 and 32 mm, respectively, to account for post-stenotic dilatation. Immediately downstream of the coarctation, a tap was placed at an angle of 60° with the centerline for Doppler ultrasound throat velocity measurements. Taps for pressure measurements were placed 2 diameters upstream of the throat of the coarctation and 10 diameters downstream of the coarctation, outside the region of pressure recovery (10). An illustration of the model is shown in Figure 1.

The models were placed in a recirculating flow system, and a transit time ultrasound flowmeter was placed upstream of the test section (Transonics, Inc., model T101). A computer-controlled flow valve generated a physiologic pulsatile flow waveform (20). The input pressure waveform was created from the average of several upstream pressure waveforms obtained by catheter from patients with coarctation.

The test fluid used was a water/glycerin mixture adjusted to match the viscosity (3.8×10^{-6} m^2/s) and density of blood at high shear rates (21). Throat velocity and pressure gradient measurements were made for flow rates from 0.5 to 5.0 liters/min, which covered a wide range of pediatric and adult cardiac output values (22). The values of nondimensional physiologic Reynolds numbers in the models ranged from 350 to 1,300. Cornstarch particles were placed in the fluid to backscatter the ultrasound beam. The throat velocities in the glass models were determined with an eight-channel pulsed Doppler ultrasound device (Instruments Development Laboratories, Baylor College of Medicine) with a theoretic sample volume height of 0.6 mm. Upstream and downstream pressure measurements were made with a solid state differential pressure transducer (Omega PX26).

In the 80% model, the maximal pressure decrease was recorded and correlated with the square of the throat velocity for pulsatile flow at several flow rates to determine the loss coefficient (equation 1). The experiments were then repeated for steady flow conditions at the peak systolic flow rate in the pulsatile flow experiments. Similar correlations were made between pressure drop and the square of the throat velocity. The steady flow results were compared with those from the pulsatile experiments to evaluate the need for pulsatile flow in further studies.

In all the models, measurements of pressure gradient versus throat velocity squared were conducted and the loss coefficients determined. These severity-based loss coefficient values were compared with the commonly used value of 4.0 mm Hg-s^2/m^2 in the simplified Bernoulli equation (10,23–32).

Imaging studies. Patients underwent imaging using the standard pediatric cardiovascular imaging protocol established at our institution. All images were obtained on a Philips Medical Systems ACS 1.5-T scanner using a quadrature body coil. After positioning the subject within the scanner, electrocardiographic (ECG) gated coronal and transverse spin echo images were obtained. The images had a slice thickness of 10.0 mm and a slice gap of 1.0 mm, and 10 slices were obtained in each orientation, which covered the entire ascending, transverse and proximal descending aorta.

To obtain MR angiographic images, a gradient–echo, "gated sweep" technique was used. The gated sweep is an inflow refreshment technique that acquires data only during a user-selectable portion of the cardiac cycle (33). By continuously exciting a slice, the signal from static tissue is suppressed, but the signal from flowing blood is bright because it enters the image during the time between excitation pulses. Hence, images show flowing blood as bright and static tissue as dark. By acquiring data only during diastole, pulsatile flow artifacts are minimized, and signal loss from post-stenotic turbulence is minimized because of lower diastolic flow. For this study, data were acquired from end-systole to 100 ms before the next r wave, as estimated from the patient's ECG tracing. The repetition time for the scan was 18.0 ms; the echo time was 6.2 ms; the flip angle was 60°; and first-order gradient moment nulling (velocity compensation) was used. The field of view for the scan was 270 mm; the scan matrix was 256×128; and two signal averages were acquired. The slice thickness for the gated sweep scan was 4.0 to 5.0 mm, and the slices overlapped by 1.0 mm. Twenty to 40 transverse slices were obtained to cover the entire aortic arch and were used to create a three-dimensional (3D) data set of the aortic arch and coarctation.

After the gated sweep scan was completed, quantitative velocity measurement was performed in the oblique sagittal plane using a phase velocity mapping sequence. The plane was set up on the spin echo and gated sweep images so that it would pass through the throat of the coarctation, which could be seen on one or both images. With the phase velocity mapping technique, imaging gradients are adjusted such that the intensity of the phase images is directly proportional to the velocity of flowing blood (34,35). The accuracy of the technique has been verified in both in vitro and in vivo studies to be 5% (35–38). Velocity measurements were taken at 16 equally spaced time points over the cardiac cycle, and two signals were averaged. The scan was performed with a field of view of 250 mm, a scan resolution 128×128 and a velocity-encoding value (maximal velocity without aliasing) of 400 to 500 cm/s.

By examining the MR angiograph and estimating the direction of the flow jet in the coarctation, the velocity-

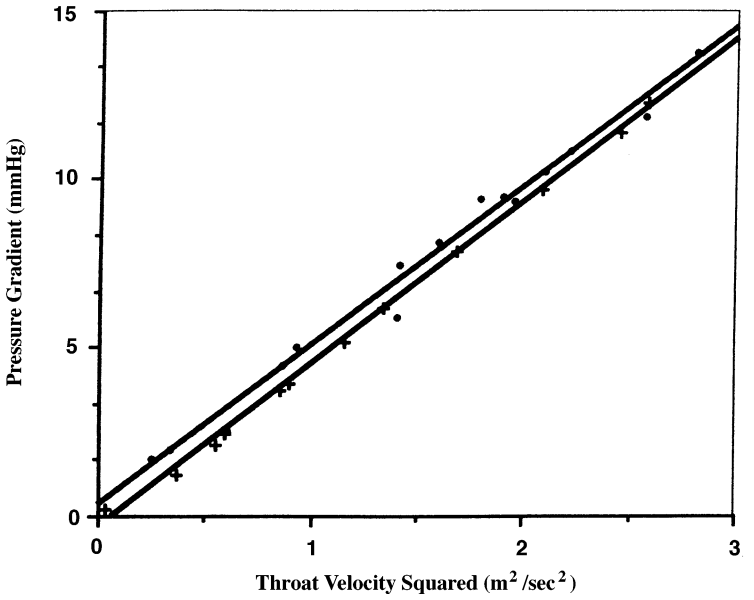

Figure 2. Comparison of pressure gradients in steady **(circles)** and pulsatile flow **(crosses)**. In the 80% model, experiments were conducted for pulsatile flow and for steady flow at the peak flow rate in pulsatile flow. Peak pressure gradient in the pulsatile flow and the pressure gradient in steady flow were correlated. The pressure gradient measurement correlated well between the steady and pulsatile flow (R = 0.98).

encoding direction (foot–head or anterior–posterior) could be chosen. The appearance of the flow jet on the velocity-encoded scans allowed determination of the angle between the velocity-encoding direction and the jet. The velocity could then be corrected by simply dividing the velocity value by the cosine of the angle between the velocity-encoding value and the direction of the jet (35).

The transverse gated sweep images were transferred to an ISG Allegro graphics workstation (ISG, Inc.) for image segmentation and 3D reconstruction. In each of the two-dimensional images, the vessel was identified by using a thresholding algorithm that segmented the vessel from the static tissue (6). This image segmentation was performed by a pediatric cardiologist (W.J.P.) experienced in interpreting MR images. After the vessel geometry was identified in the transverse images, the aorta was constructed into a single 3D object. The program allowed rotation of the object in any direction and allowed measurements to be made on the object. From the 3D object, a measure of the stenosis severity was made by measuring the vessel diameter at the throat of the coarctation and at a point proximal to the coarctation.

Patients. A series of 32 consecutive patients (mean age 10.5 years, range 1 to 23) who were referred to our institution for evaluation of aortic coarctation with MRI from November 1993 to August 1995 were included in the study. All patients were status postsurgical repair of the coarctation. The repairs included patch grafts, tube grafts, subclavian flap repairs or balloon dilation. The timing of the MRI examination after the operation varied from 1 month to 11 years.

In 22 of the patients, Doppler ultrasound estimates of the pressure gradient were available and were compared with those from MRI estimates. Doppler ultrasound examinations were done at our institution on a Hewlett-Packard Sonos 2000 using a 2.7/3.5-MHz transthoracic transducer or in the office of the referring physician. A loss coefficient of 4.0 was used to estimate pressure. In all cases but one, the ultrasound examination was done within 1 month of the MRI examination. In the one exception, the Doppler examination was done within 6 months of the MRI examination.

In six patients, cardiac catheterization was performed by standard techniques using a Berman 5F catheter, and the pressure gradient across the coarctation was measured. In all cases, the catheter pressure measurement was done at our institution.

Results

Model studies. Correlations of pressure gradient as a function of the square of the throat velocity were made at the peak flow value during pulsatile flow and during steady flow at the peak value in the 80% coarctation model. The peak pressure gradients during pulsatile flow showed no significant difference with steady flow at the peak flow value for slope, y-intercepts or regression coefficients. Figure 2 illustrates pressure gradient versus throat velocity squared for steady and pulsatile flow conditions. There was no significant difference between the pressure versus velocity-squared relation for the steady and pulsatile flow data ($p < 0.05$ for the slopes of the lines in Fig. 3 using a Student t test). Thus, flow conditions could be fully modeled with steady flow. Pressure gradient versus velocity-squared measurements for the 50%, 55%, 60%, 70% and 90% stenoses were performed under steady flow conditions only.

The loss coefficient K, defined as the ratio of pressure gradient to the square of the throat velocity, was found to be a function of flow rate and percent stenosis (Fig. 3). It was observed that the loss coefficient approached a value of 4.0 mm

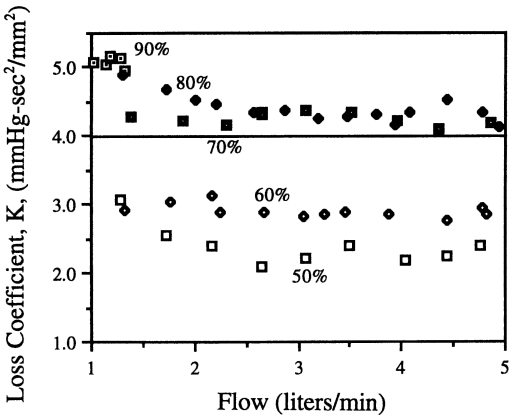

Figure 3. Loss coefficient plotted versus flow rate for all models. The value of the loss coefficient varied with flow rate at low flow values. However, for flow rates >1.5 liters/min, the loss coefficient was constant. For models with severity less than ~65%, the loss coefficient was <4.0. For models with severity greater than ~65%, the loss coefficient was >4.0.

Figure 4. Three-dimensional reconstruction of an aorta with a coarctation. A 3D image of the aorta was created for all the patients. The 3D image was created from the set of multiple transverse images obtained with the gated inflow technique. The aorta was segmented out in each individual image by a pediatric cardiologist (W.J.P.). The 3D image of the aorta was then created from the segmented images by an image processing program (ISG Allegro, Toronto, Ontario, Canada).

Hg-s^2/m^2 for moderate flow through the 65% to 70% stenosis model. Although the loss coefficient varied with flow rate in every model, it was constant for flow rates >1.5 liters/min. Because the loss coefficient is a strong function of percent stenosis, percent stenosis should be determined before estimating the pressure drop in a patient.

Pressure gradient versus the square of the throat velocity was plotted for each individual model, and the loss coefficient (slope of the line) was determined for each model. Table 1 lists the loss coefficients for the various values of stenosis severity. The loss coefficient was <4.0 mm Hg-s^2/m^2 in the models with stenoses less severe than 70%. For a stenosis with a severity of 90%, the loss coefficient was 4.9 mm Hg-s^2/m^2.

Patient studies. In all patients, the coarctation was successfully visualized on the spin echo and gated sweep images. A 3D image was reconstructed from the gated sweep images, Figure 4 illustrates an aortic coarctation in one of the patients (arrow shows coarctation location). The measurements of stenosis severity were taken as the smallest dimension on the 3D objects and compared with the nominal upstream diameter to calculate stenosis severity. The phase velocity scan was successful in 29 of 32 patients. One of the three patients with an unsuccessful scan presented with confusing geometry, and velocity was encoded in the incorrect direction. The other two patients had moved during the phase velocity scan. Figure 5A illustrates the slice location of a phase velocity scan superimposed on a transverse spin echo image (arrows show slice location). Figure 5B illustrates a phase velocity map at peak systole from one of the patients (arrows show location of increased velocity). From these images, the peak throat velocity in the coarctation was obtained using software available on the scanner. Using the peak systolic throat velocity measurements and the stenosis severity measurements, pressure gradients were calculated.

Table 1. Stenosis Severity-Based Coefficients Versus Loss Coefficients Determined From Laboratory Model Studies

Stenosis Severity (mm Hg-s^2/m^2)	Loss Coefficient (mm Hg-s^2/m^2)
50%	2.3
55%	2.8
60%	2.9
70%	4.2
80%	4.3
90%	4.9

A computer program was created to determine the pressure gradient for a given stenosis severity and throat velocity. This program used the loss coefficient values obtained in the laboratory portion of the experiments. Once the throat velocity was entered, the program linearly interpolated between loss coefficient values to provide severity-based estimates of pressure gradients across coarctations.

Table 2 presents patient data and pressure gradients in the 32 patient studies calculated from the MR phase velocity maps with the severity-based loss coefficients determined in the model study and with the commonly used value of 4.0. The error in determining the peak systolic pressure gradient using a loss coefficient K of 4.0, compared with the severity-based coefficients, ranged from 1 to 18 mm Hg. In 22 patients an estimate of peak systolic pressure gradient was available from an ultrasound examination, and these data are also presented in Table 2. In six patients, these data were available from pressure gradient measurement during catheterization and are also presented in Table 2.

The ultrasound estimates of pressure gradient are plotted

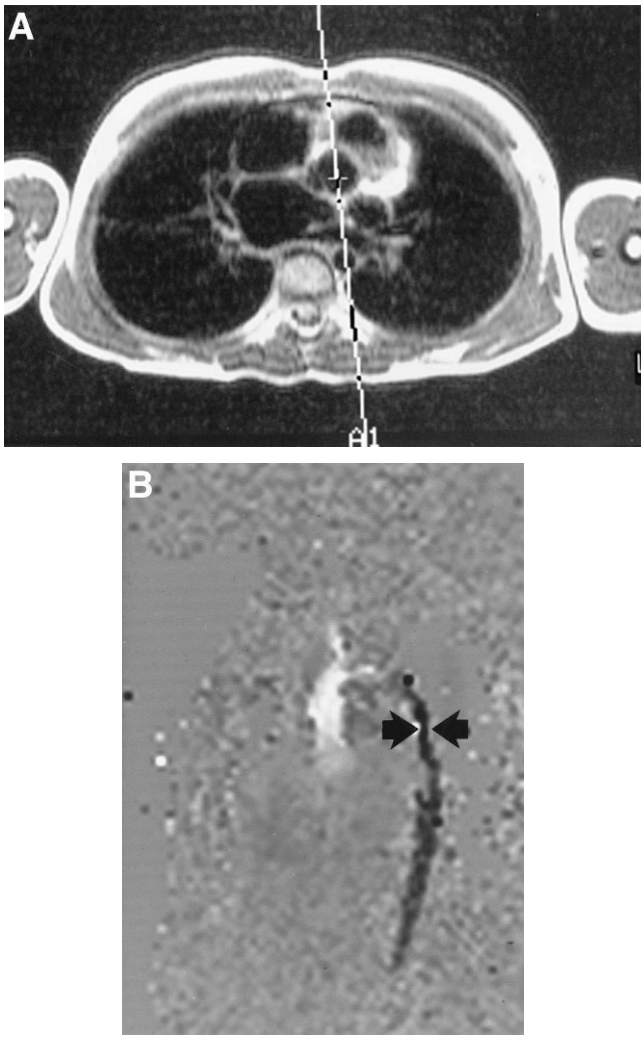

Figure 5. Magnetic resonance phase velocity map through the throat of a coarctation. The velocity image was planned through the throat of the coarctation on the transverse spin echo image (**A**). In the phase velocity map (**B**), image intensity is directly proportional to velocity. The bright signal in the ascending aorta indicates rapid flow toward the head; the dark signal in the descending aorta indicates rapid flow toward the feet. **Arrows** indicate the location of the coarctation where a local increase in velocity is seen.

against the MRI pressure gradient estimates calculated using a loss coefficient of 4.0 (for both techniques) in Figure 6. The graph indicates excellent correlation between the two methods ($R = 0.91$). In 19 of the 22 patients with available ultrasound examination results, MRI pressure gradient estimates agreed with ultrasound to within 10%. In three cases, MRI estimates of pressure gradient were lower than those of ultrasound (by >10%). This graph indicates that MRI pressure gradient estimates using a loss coefficient of 4.0 agrees well with Doppler ultrasound, indicating that the techniques are similar for measuring stenotic throat velocities. However, Table 2 shows that MRI can make pressure gradient measurements that are improved over ultrasound by using severity-based loss coefficients.

Table 2. Patient Data and Pressure Gradients

		Peak Systolic Pressure Gradient (mm Hg)			
Pt No./ Age (yr)	Severity (by diam)	MR (K = 4)	MR (K severity based)	Doppler Ultrasound (K = 4)	Invasive Catheter
1/0	0.67	24	23	25	
2/8	0.47	33	16*	—	
3/5	Exam failed—incorrect velocity encoding			8	
4/7	0.55	14	10*	28	
5/16	Exam failed—patient moved			—	
7/18	0.48	27	14*	—	
7/11	0.47	20	10**	—	
9/5	0.65	42	40	48	38
10/1	0.45	23	11*	—	
11/14	0.43	27	10*	30	10
12/7	0.45	29	14	—	22
13/11	0.64	49	42	46	
14/14	0.67	55	53	—	
15/12	0.50	29	16*	36	
16/20	0.65	44	42	—	
17/10	0.53	25	17	25	
18/23	0.60	27	15	25	
19/5	0.63	38	32	38	
20/15	0.55	35	25	30	10
21/2	0.22	0	0	0	
22/7	0.23	0	0	0	
23/11	0.44	15	7	—	
24/13	0.65	20	18	—	
25/1	0.65	49	47	50	
26/10	0.25	0	0	0	
27/10	0.45	23	12*	25	
28/14	Exam failed—patient moved			—	
29/18	0.44	23	10*	20	
30/15	0.65	23	21	—	20
31/21	0.40	11	3	—	
32/4	0.45	23	11*	26	5

*Severity-based loss coefficient differed from value obtained with K = 4 by >40%. diam = diameter; Exam = examination.

Figure 7 plots the pressure gradient averaged over all subjects who had all three examinations: 1) MRI with the severity-based loss coefficient; 2) Doppler ultrasound; and 3) cardiac catheterization. Figure 7 shows that MRI estimates made using the severity-based loss coefficient and catheterization pressure measurements are both significantly lower than those of ultrasound ($p < 0.05$). If the catheterization pressure gradient measurements are taken as the reference standard, Figure 8 shows that the MRI pressure gradient measurements made using the severity-based loss coefficients agree well with catheterization pressure measurements (difference not significant at $p < 0.05$), and MRI measurements are more accurate than those measurements made with Doppler ultrasound.

Discussion

The results of the present study indicate that a combination of MRI and MR phase velocity measurements can accurately

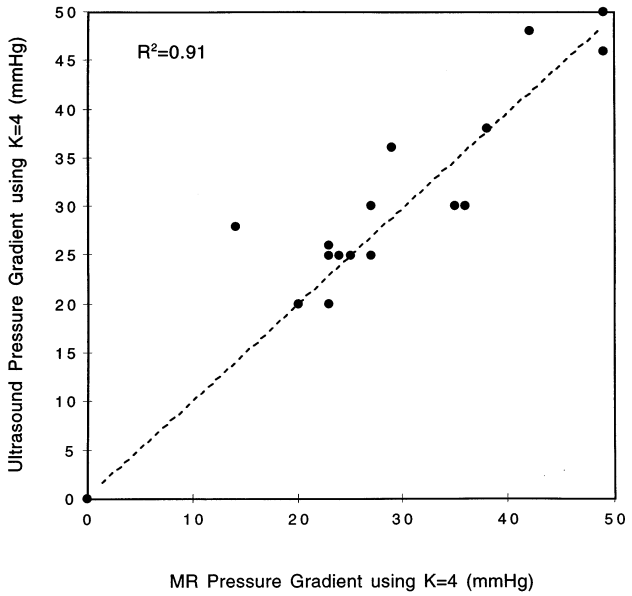

Figure 6. Correlation of the MRI and Doppler ultrasound pressure gradient estimates. In the 22 patients with available Doppler ultrasound estimates of pressure gradient, the MRI pressure gradients calculated with a loss coefficient of 4.0 are plotted against the ultrasound estimates. Correlation between the two methods was excellent (R = 0.91). In 19 of the 22 patients, the MRI and ultrasound estimates were within 10%, indicating that MRI using a loss coefficient of 4.0 provides pressure gradient estimates comparable to ultrasound. However, using severity-based loss coefficients, MRI results in improved estimates of pressure gradient.

determine pressure gradients across coarctations by determining both stenosis severity and throat velocity. Because the loss coefficient is a strong function of stenosis severity, the percent stenosis should be known before estimating the pressure decrease in a patient. By using severity-based loss coefficients, MRI can make pressure gradient measurements that are more accurate than estimates that simply assume a constant loss coefficient of 4.0. Magnetic resonance imaging offers a complete noninvasive examination of aortic coarctation because stenosis location and severity can be determined with angiographic sequences, and the pressure gradient can be determined with MR phase velocity mapping. In addition, the inherent 3D nature of MR angiography is a useful tool for surgical planning.

Model studies. The laboratory studies showed that in mild stenoses (<60%), using a loss coefficient of 4.0 tended to overestimate the pressure gradient. In mild (<60%) stenoses, the discrepancy between using a loss coefficient of 4.0 and a severity-based loss coefficient is due to the proximal velocity being ignored and to the pressure recovery distal to the stenosis. In severe stenoses, the upstream velocity can be neglected, but the pressure losses from turbulence cause an extended pressure drop that extends downstream of the coarctation. This increased pressure loss will cause underestimation of the pressure gradient when applying the simplified Bernoulli equation.

In stenoses with severities near 65%, the effects of overestimation of pressure gradients in mild stenoses and underestimation of pressure gradients in severe stenoses counteract each other such that the simplified Bernoulli equation accurately estimates the pressure drop. Our experimental results agree with previous fluid mechanical analyses of stenotic pressure gradients and previous analyses of the Bernoulli equation that show the same results (9,10).

As mentioned earlier, in addition to stenosis severity, the

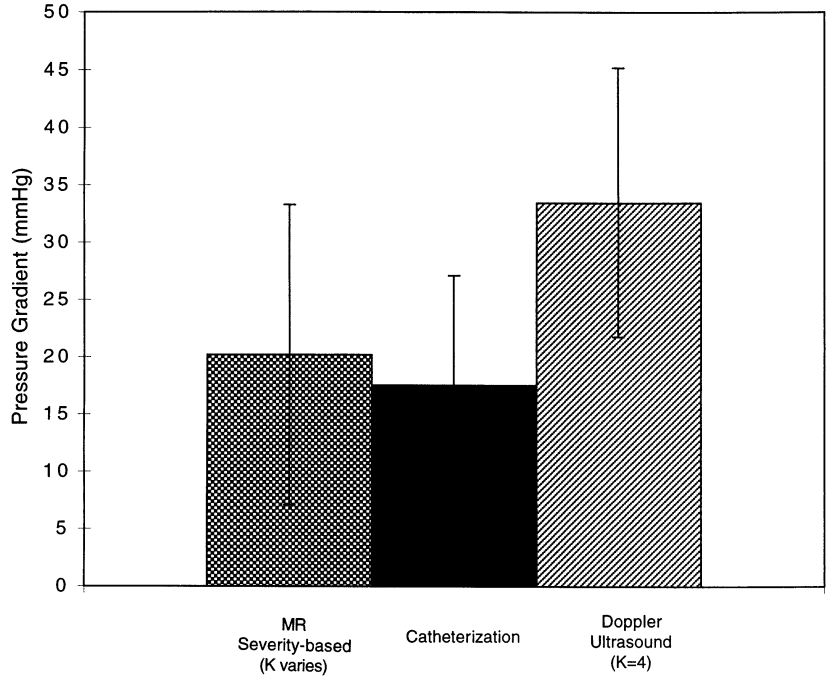

Figure 7. Pressure gradient values from patients who had all three examinations (MRI, Doppler ultrasound, catheterization). Pressure gradient was determined by 1) MRI using severity-based loss coefficients; 2) Doppler ultrasound; and 3) cardiac catheterization. The values of pressure gradient calculated with MRI using the severity-based loss coefficient were less than those estimated with Doppler ultrasound (20 vs. 34, $p < 0.05$). The MRI pressure gradient estimates made with the severity-based loss coefficients agree well with catheterization values (20 vs. 18, no significant difference, $p = 0.05$). Hence, use of the severity-based loss coefficients will result in a more accurate estimate of pressure gradient.

shape of the stenosis can have an effect on the values of the loss coefficients. For this study we used a model that was derived from a series of angiograms of aortic coarctations. Therefore, the shape represented the characteristic "pinch" geometry of an aortic coarctation. Although the loss coefficients determined in this study could be applied to other geometries, the values determined were for aortic coarctation geometries only.

The shape of the loss coefficient curves as a function of flow rate (Fig. 2) can be explained by the principles of fluid mechanics. In general, for high flow rates, turbulent pressure losses are proportional to the square of velocity; consequently, the loss coefficient is constant (39). For low flow rates, pressure loss increases linearly with velocity, and the loss coefficient is inversely proportional to the flow rate (39). However, because the loss coefficient is constant with the flow rate for values >1.5 liters/min, variation with flow rate can be ignored in most cases.

Patient studies. The MR phase velocity mapping studies conducted in patients to determine coarctation throat velocity and to estimate pressure gradient show that the use of 4.0 as a loss coefficient for a wide range of stenoses can lead to errors in estimating gradients. Errors up to 17 mm Hg were seen in the patients examined. This error could be large enough to affect clinical decisions.

Comparison between the pressure estimates obtained with MRI and ultrasound in patients implies that the use of a loss coefficient of 4.0 can lead to significant errors in pressure gradient estimates. In one patient with a 45% stenosis, ultrasound estimated a pressure gradient of 30 mm Hg (using a loss coefficient of 4.0), and MRI estimated a pressure gradient of 10 mm Hg using the severity-based loss coefficient. The pressure measurement at catheterization was also 10 mm Hg.

One limitation of the patient studies is that no severe coarctations (>70%) were included in the study. At our institution, patients who have a severe coarctation are not evaluated with MRI; they are taken directly to the operating room. Hence, inclusion in our study of patients with mild and moderate coarctation was dictated by clinical practice. A second limitation is that invasive catheter pressure gradient measurements were obtained to compare with MRI pressure gradient estimates in only six patients. However, if the catheter pressure gradient measurements are assumed to be the reference standard, the findings in these six patients do support the conclusion that use of the severity-dependent loss coefficients provides a more accurate measurement of pressure gradient than use of a loss coefficient of 4.0.

Although MRI velocity measurements have been verified in a number of in vitro and in vivo studies, there are several errors that can affect the accuracy of the phase velocity measurements, including off-axis velocity measurements, finite pixel size and turbulent signal loss (35–38,40). In the present study, we acquired scout images in several orientations to ensure that the phase velocity measurements were performed directly through the throat of the stenosis with the jet velocity in-plane. The voxel size for these measurements was $2 \times 2 \times 5$ mm, which was chosen to balance resolution and signal to noise factors. For pediatric aortas (~12 to 15 mm), this voxel size was sufficient to resolve jet velocities. By using a slice that was in the plane of the aorta, the problem of turbulent signal loss did not significantly affect the measurements. There was turbulent signal loss in several of the patients, but it was downstream of the coarctation. Proximal to the stenosis and in the throat of the stenosis, signal was preserved, and velocity measurements of stenosis severity could be made.

Three-dimensional reconstruction of the anatomy of the coarctation proved particularly helpful to surgeons and referring physicians. In addition to showing the exact location and severity of the coarctation, 3D reconstruction showed the specific shape of the lesion, allowed visualization of collateral vessels and elucidated the degree of post-stenotic dilation.

Conclusions. We showed that use of severity-based loss coefficients allows more accurate determination of the pressure gradient across stenoses. Use of MRI and MR phase velocity mapping can allow complete evaluation of aortic coarctation by determining stenosis location, stenosis severity and pressure gradient across the stenosis, yielding a 3D image of the aorta for operation.

References

1. Campbell M. Natural history of coarctation of the aorta. Br Heart J 1970;32:633–40.
2. Rao PS, Gala LO, Smith PA, Wilson AD. Five- to nine-year follow-up results of balloon angioplasty of native aortic coarctation in infants and children. J Am Coll Cardiol 1996;27:462–70.
3. Rees S, Somervill J, Ward C, et al. Coarctation of the aorta: MR imaging in late postoperative assessment. Radiology 1989;173:499–502.
4. Boxer RA, LaCorte MA, Singh S, Cooper R, Goldman MM, Stein HL. Nuclear magnetic resonance imaging in evaluation follow-up of children treated for coarctation of the aorta. J Am Coll Cardiol 1986;7:1095–8.
5. Pucillo AL, Schechter AG, Kay RH, Herman MV. Magnetic resonance imaging of vascular conduits in coarctation of the aorta. Am Heart J 1989;117:482–5.
6. Parks WJ, Ngo TD, Plauth WH, et al. Incidence of aneurysm formation after Dacron patch aortoplasty repair for coarctation of the aorta: long-term results and assessment utilizing magnetic resonance angiography with three-dimensional surface rendering. J Am Coll Cardiol 1995;26:266–71.
7. Nyman R, Hallberg M, Sunnegardh J, Thuren J, Henze A. Magnetic resonance imaging and angiography for the assessment of coarctation of the aorta. Acta Radiol 1989;30:481–5.
8. Simpson IA, Chung KJ, Glass RF, Sahn DJ, Sherman FS, Hesselink J. Cine magnetic resonance imaging for evaluation of anatomy and flow relations in infants and children with coarctation of the aorta. Circulation 1988;78: 142–8.
9. Marx GR, Allen HD. Accuracy and pitfalls of Doppler evaluation of the pressure gradient in aortic coarctation. J Am Coll Cardiol 1986;7:1379–85.
10. Rijsterborgh H, Roeland J. Doppler assessment of aortic stenosis: Bernoulli revisited. Ultrasound Med Biol 1987;13:241–8.
11. Yoganathan AP, Valdes-Cruz LM, Schmidt-Dohna J, et al. Continuous-wave Doppler velocities and gradients across fixed tunnel obstructions: studies in vitro and in vivo. Circulation 1987;76:657–66.
12. Levine RA, Jimoh A, Cape EG, McMillian S, Yoganathan AP, Weyman AE. Pressure recovery distal to a stenosis: potential cause of gradient overestimation by Doppler echocardiography. J Am Coll Cardiol 1989;13:706–15.
13. Young DF, Tsai FY. Flow characteristics in models of arterial stenoses—I. steady flow. J Biomech 1973;6:395–410.
14. Muligan SA, Doyle M, Matsuda T, et al. Aortoiliac disease: two-dimensional inflow angiography with lipid suppression. J Magn Reson Imaging 1993;3: 829–34.
15. Kent KC, Edelman RR, Kim D, Steinman TI, Porter DH, Skillman JJ.

Magnetic resonance imaging: a reliable test for the evaluation of proximal renal arterial stenosis. J Vasc Surg 1991;13:311–8.
16. Anson JA, Heiserman JE, Drayer BP, Spetzler RF. Surgical decision on the basis of magnetic resonance angiography of the carotid arteries. Neurosurgery 1993;32:335–43.
17. Stern HC, Locher D, Wallnofer K, et al. Noninvasive assessment of coarctation of the aorta: comparative measurements by two-dimensional echocardiography, magnetic resonance, and angiography. Pediatr Cardiol 1991;12:1–5.
18. Sondergaard L, Hidebrandt P, Lindvig K, et al. Valve area and cardiac output in aortic stenosis: quantification by magnet resonance velocity mapping. Am Heart J 1993;127:1156–64.
19. Kilner PJ, Manzara CC, Mohiaddin RH, et al. Magnetic resonance jet velocity mapping in mitral and aortic valve stenosis. Circulation 1993;87:1239–48.
20. Moore JE, Ku DN, Glagov S, Zarin CK. Pulsatile flow visualization in the abdominal aorta: implications for increased susceptibility to atherosclerosis. J Biomech Eng 1992;114:391–7.
21. Fung YC. Biomechanics. New York: Springer-Verlag, 1988:63–5.
22. Guyton AC. Textbook of Medical Physiology. 8th ed. Philadelphia: WB Saunders, 1991.
23. Weber G, Strauss AL, Rieger H, Scheffler A, Eisenhoffer J. Validation of Doppler measurement of pressure gradient across a peripheral model arterial stenosis. J Vasc Surg 1992;16:10–6.
24. Hattle L. Noninvasive assessment and differentiation of left ventricular outflow obstruction with Doppler ultrasound. Circulation 1981;64:381–7.
25. Faccenda F, Usui Y, Spencer MP. Doppler measurement of the pressure drop caused by arterial stenosis: an experimental study. Angiology 1985;36: 899–905.
26. Cape EG, Yoganathan AP, Levine RA. A new theoretical model for noninvasive quantification of mitral regurgitation. J Biomech 1990;23:27–33.
27. Kosturakis D, Allen HD, Goldberg SJ, Sahn DJ, Valdez-Cruz LM. Noninvasive quantification of stenotic semilunar valve areas by Doppler echocardiology. J Am Coll Cardiol 1984;3:1256–62.
28. Yeager M, Yock PG, Popp RL. Comparison of Doppler derived pressure gradient to that determined at cardiac catheterization in adults with aortic stenosis: implications for management. Am J Cardiol 1986;57:644–8.
29. Currie PJ, Seward JB, Reeder GS, et al. Continuous-wave Doppler echocardiographic assessment of severity of calcific aortic stenosis: a simultaneous Doppler-catheter correlative study in 100 adult patients. Circulation 1985;71:1162–9.
30. Zhang Y, Ihlen H, Nitter-Hauge S. Estimation of peak-to-peak pressure gradient in aortic stenosis by Doppler echocardiography. Int J Cardiol 1986;10:197–212.
31. Berger M, Berdorf RL, Galterstein PE, Goldberg E. Evaluation of aortic stenosis by continuous wave Doppler ultrasound. J Am Coll Cardiol 1984; 3:150–6.
32. Stevenson JG, Kawabori I. Noninvasive determination of pressure gradients in children: two methods employing pulsed Doppler echocardiography. J Am Coll Cardiol 1984;3:179–92.
33. de Graaf RG, Groen JP. MR angiography with pulsatile flow. Magn Reson Imaging 1992;10:25–34.
34. van Dijk P. Direct cardiac NMR imaging of heart wall and blood flow velocity. J Comput Assist Tomogr 1984;8:429–36.
35. Firmin DN, Nayler GL, Kilner PJ, Longmore DB. The application of phase shifts in NMR for flow measurement. Magn Reson Med 1990;14:230–41.
36. Oshinski JN, Ku DN, Bohning DA, Pettigrew RI. The effect of acceleration on the accuracy of phase velocity mapping in accelerating flows. J Magn Reson Imaging. 1992;2:665–70.
37. Pettigrew RI, Daniels W, Galloway JR. Quantitative phase flow MR imaging in dogs by using standard sequences: comparison with in vivo flow meter measurements. AJR Am J Roentgenol 1987;148:411–4.
38. Buonocore MH, Bogren H. Factors influencing the accuracy and precision of velocity-encoded phase imaging. Magn Reson Med 1992;26:141–54.
39. Ku DN, Klafta JM, Gewertz BL, Zarins CK. The contribution of valves to saphenous vein graft resistance. J Vasc Surg 1987;6:274–9.
40. Oshinski JN, Pettigrew RI, Ku DN. Turbulent fluctuation velocity: the most significant determinate in post-stenotic signal loss. Magn Reson Med 1995;33:193–9.